Synthesis and Excited State Dynamics of μ-Oxo Group IV Metal Phthalocyanine Oligomers: Trimers and Tetramers

Tissa Gunaratne,[†] Vance O. Kennedy,[‡] Malcolm E. Kenney,*[,‡] and Michael A. J. Rodgers*[,†]

Center for Photochemical Sciences and Department of Chemistry, Bowling Green State University, Bowling Green, Ohio 43403 and Department of Chemistry, Case Western Reserve University, Cleveland, Ohio 44106

Received: December 12, 2003; In Final Form: February 9, 2004

Two μ-oxo silicon phthalocyanines have been synthesized and subjected to photophysical examination. The results have been compared to the monomeric and dimeric systems published previously. The Q-bands in the ground state absorption spectra undergo a blue shift with respect to the monomer due to an excitonic interaction of the transition dipoles of the coplanar silicon phthalocyanine units having central symmetry along the Si−O−Si axis, with no significant molecular orbital overlap. This excitonic interaction generates a new set of excited states. The Q-band shift (with respect to the monomer) is greater as the number of phthalocyanine rings is increased consistent with the molecular exciton model of a linear polymer. On suprananosecond time scales, photoexcitation generated optical absorptions of triplet states that decayed with intrinsic lifetimes in the tens of microseconds region. These were quenched in the presence of O_2 with bimolecular rate constants for the trimer and tetramer of near 2×10^6 M^{-1} s^{-1}, indicating that the T_1 states of the trimer and tetramer lie significantly below the energy of the $^1\Delta_g$ state of oxygen (22.5 kcal mol^{-1}). Estimates of the energy of T_1 generated values of approximately 17 kcal mol^{-1} for both compounds, some 2 kcal mol^{-1} lower than that calculated for the dimer. Photon absorption results in the formation of the highest lying exciton state, which deactivates to the lowest exciton state, which subsequently undergoes intersystem crossing to the triplet manifold. The ultrafast pump−probe results demonstrated that part of the lowest exciton state population was complete within the instrument rise time, whereas other populations required several picoseconds to develop, probably on account of the requirement for torsional/vibrational relaxation of excited state populations produced from ground state molecules having lower symmetry than D_{4h}.

Introduction

Silicon phthalocyanine is capable of forming stacked μ-oxo oligomeric structures in which the stacking axis, formed by Si−O−Si−O− bonds, is orthogonal to the phthalocyanine π-planes. These μ-oxo oligomers have been considered very useful in developing molecular electronic devices due to their superior physical and chemical stability and have shown promising applicability in fabricating planer photodiodes and sensors.[1,2] They have also proved to be useful as nonlinear optical materials that are excellent candidates for optical switching and optical limiting applications.[3]

The most observable difference between the monomer and the oligomers is in the UV−visible absorption spectra in a solvent like toluene, where the oligomers spectra show significant blue shift in the long wavelength band, and this shift increases with the number of monomer units. This blue shift arises from the splitting of the normally degenerate orbital of the separated monomer under the influence of the two co-facially stacked π-orbitals.[4] The first excited state is therefore composed of a pair of excitonic states that are different in energy by an amount that depends on the interplanar spacing and number of monomer units. The upper excitonic state, $|+\rangle$, is optically allowed, and optical transitions originating from the ground state populate the upper excitonic state, resulting in the spectral blue shift. The excited upper excitonic state rapidly deactivates to the lower excitonic state, $|-\rangle$, for which the pure electronic transition to the ground state is forbidden.[1] Very weak and highly red shifted fluorescence has been reported for the μ-oxo dimer,[5] but no fluorescence has been reported for the trimer and tetramer. Excited state dynamics of the μ-oxo dimer has been extensively studied using nanosecond[1] and ultrafast[6] transient absorption spectroscopy and exciton migration in the polymeric species (phthalocyaninato)polysiloxane using ultrafast transient spectroscopy has also been reported.[7]

Very recently this laboratory and collaborators have been investigating the feasibility of using intense photothermal effects in cellular milieux as a modality for means of inducing cell necrosis; so-called photothermal therapy (PTT). This depends critically on photosensitizer compounds being capable of very rapid electronic-to-vibrational energy degradation within their excited state manifold. This generates a thermal spike that dissipates and in so doing causes major damage to the surrounding biosystems.[8]

It has been demonstrated that aggregated photosensitizers are more efficient in this than isolated molecules and this leads to the idea of using covalently linked oligomeric/polymeric species as PTT photosensitizers, rather than relying on adventitious aggregation of molecular units in the required site. As a first attempt in this arena, here we report the photodynamic properties of two μ-oxo silicon phthalocyanine oligomers, the trimer and

* Corresponding authors. E-mail: M.A.J.R., rodgers@bgnet.bgsu.edu; M.E.K., malcolm.kenney@case.edu.
[†] Bowling Green State University.
[‡] Case Western Reserve University.

10.1021/jp037846k CCC: $27.50
Published on Web 03/12/2004

the tetramer. The excited state dynamics of μ-oxo oligomers having more than two monomeric units have not been reported to date and the present study focuses on these properties of the μ-oxo trimer and tetramer species in an effort to understand the excited state behavior with increasing monomer units.

Experimental Procedures

Synthesis. *Materials.* The reagents and solvents were from commercial vendors.

*HO(SiPcO)$_n$H, **1***. The route used to prepare HO(SiPcO)$_n$H and the other oligomers is based on previous work.[9,10]

A mixture of $SiPcCl_2$ (1.11 g), $SiPc(OH)_2$ (1.47 g), quinoline (dry, 70 mL), and tri-*n*-butylamine (6.0 mL) was refluxed under Ar for 1 h, cooled (ice bath), treated over 3 h with HCl (concentrated, 15 mL), diluted with CH_3OH (50 mL), and filtered, and the solid was washed (CH_3OH). A cooled (ice bath) mixture of the washed solid and H_2SO_4 (concentrated, 80 mL) was stirred for 3 h, mixed with an ice−H_2O slurry (600 mL), and filtered. A mixture of the solid thus isolated and an ammonium hydroxide−pyridine solution (1:1 200 mL) was stirred for 3 h, diluted with H_2O (100 mL), settled for 2 days, and filtered. The solid obtained was washed (H_2O, acetone, toluene, hexanes), vacuum-dried (70 °C), and weighed (2.40 g).

The product is a blue solid. It is insoluble in dimethylformamide, CH_2Cl_2, toluene, and hexanes.

*(n-C$_6$H$_{13}$)$_3$SiO(SiPcO)$_n$Si(n-C$_6$H$_{13}$)$_3$, **2***. A mixture of HO(SiPcO)$_n$H (2.40 g), tri-*n*-hexylchlorosilane (8.0 mL), and a toluene−pyridine solution (2:1, 150 mL) was refluxed under Ar for 5 h and filtered. The solid was washed (toluene), and the washings and filtrate were combined and evaporated to near dryness by rotary evaporation. The solid was weighed (1.95 g). The product is an oily blue solid.

*(n-C$_6$H$_{13}$)$_3$SiOSiPcOSi(n-C$_6$H$_{13}$)$_3$, **3***. (*n*-C_6H_{13})$_3$SiO(SiPcO)$_n$Si(*n*-C_6H_{13})$_3$ (1.00 g) was chromatographed (5:1 hexanes−toluene solution, Al_2O_3 III, 50:1 hexanes−toluene solution), and the solid obtained was vacuum-dried (70 °C) and weighed (116 mg). UV−vis (toluene), λ_{max}/nm (log ϵ): 669 (5.6). NMR (300 MHz, C_6D_6): δ 9.74 (m, 8H, 1,4-Pc H), 7.91 (m, 8H 2,3-Pc H), 0.95 (m, 12H, $SiC_4H_8CH_2$), 0.80 (t, 18H, $SiC_5H_{10}CH_3$), 0.53 (m, 12H, $SiC_3H_6CH_2$), 0.24 (m, 12H, $SiC_2H_4CH_2$), −0.96 (m, 12H, $SiCH_2CH_2$), −2.09 (m, 12H, $SiCH_2$). The monomer is a blue solid. It is soluble in CH_2Cl_2 and toluene, slightly soluble in hexanes and insoluble in dimethylformamide.

*(n-C$_6$H$_{13}$)$_3$SiO(SiPcO)$_2$Si(n-C$_6$H$_{13}$)$_3$, **4***. (*n*-C_6H_{13})$_3$SiO(SiPcO)$_n$Si(*n*-C_6H_{13})$_3$ was chromatographed further (10:1 hexanes−toluene solution), and the solid obtained was vacuum-dried (70 °C) and weighed (467 mg). UV−vis (toluene), λ_{max}/nm (log ϵ): 632 (5.5). NMR (300 MHz, C_6D_6): δ 9.24 (m, 16H, 1,4-Pc H), 8.06 (m, 16H, 2,3-Pc H), 0.59 (m, 30H, overlapping $SiC_4H_8CH_2$ and $SiC_5H_{10}CH_3$), 0.04 (m, 12H, $SiC_3H_8CH_2$), −0.39 (m, 12H, $SiC_2H_4CH_2$), −1.92 (m, 12H, $SiCH_2CH_2$), and −3.15 (m, 12H, $SiCH_2$). The dimer is a blue solid. It is soluble in CH_2Cl_2 and toluene, slightly soluble in hexanes, and insoluble in dimethylformamide.

*(n-C$_6$H$_{13}$)$_3$SiO(SiPcO)$_3$Si(n-C$_6$H$_{13}$)$_3$, **5***. (*n*-C_6H_{13})$_3$SiO(SiPcO)$_n$Si(*n*-C_6H_{13})$_3$ was chromatographed still further (1:1 hexanes−toluene solution), and the solid was vacuum-dried (70 °C) and weighed (122 mg). UV−vis (toluene), λ_{max}/nm (log ϵ): 620 (5.4). NMR (300 MHz, C_6D_6): δ 8.80 (m, 16H, terminal 1,4-Pc H), 8.73 (m, 8H, middle 1,4-Pc H), 8.20 (m, 8H, middle 2,3-Pc H), 7.83 (m, 16H, terminal 2,3-Pc H), 0.40 (m, 30H, overlapping $SiC_4H_8CH_2$ and $SiC_5H_{10}CH_3$), −0.25 (m, 12H, $SiC_3H_6CH_2$), −0.67 (m, 12H, $SiC_2H_4CH_2$), −2.36 (m, 12H, $SiCH_2CH_2$), −3.63 (m, 12H, $SiCH_2$). The trimer is a blue solid. It is soluble in CH_2Cl_2 and toluene, very slightly soluble in hexanes, and insoluble in dimethylformamide.

*(n-C$_6$H$_{13}$)$_3$SiO(SiPcO)$_4$Si(n-C$_6$H$_{13}$)$_3$, **6***. (*n*-C_6H_{13})$_3$SiO(SiPcO)$_n$Si(*n*-C_6H_{13})$_3$ was chromatographed further yet (toluene), and the solid obtained was vacuum-dried (70 °C) and weighed (148 mg). UV−vis (toluene), λ_{max}/nm (log ϵ): 616 (5.3). NMR (300 MHz, C_6D_6): δ 8.52 (m, 16H, terminal 1,4-Pc H), 8.30 (m, 16H, middle 1,4-Pc H), 8.01 (m, 16H, middle 2,3-Pc H), 7.63 (m, 16H, terminal 2,3-Pc H), 0.40 (m, 30H, overlapping $SiC_4H_8CH_2$ and $SiC_5H_{10}CH_3$), −0.25 (m, 12H, $SiC_3H_6CH_2$), −0.69 (m, 12H, $SiC_2H_4CH_2$), −2.36 (m, 12H, $SiCH_2CH_2$), −3.66 (m, 12H, $SiCH_2$). The tetramer is a blue solid. It is soluble in CH_2Cl_2 and toluene, and insoluble in dimethylformamide and hexanes. Structures are shown in Figure 1.

NMR Spectra. The NMR spectra were recorded with a Varian Gemini 300 spectrometer.

UV−Visible Absorption Spectra. The ground state absorption spectra were recorded for monomer through tetramer in solutions of 2−3 μM in toluene using a Varian Cary 50 Bio spectrophotometer. The extinction coefficients for the monomer through the tetramer were calculated from data obtained with a Perkin-Elmer Lambda 25 spectrometer.

Transient Absorption Spectra and Kinetics. Transient spectra were recorded in deaerated solutions in toluene by bubbling the sample with argon for several minutes in a cuvette with a Teflon cap equipped with a hypodermic syringe and a small hole to allow egress of gas. The excitation beam was obtained from a Surelite I (Continuum) Q-switched Nd:YAG laser with ca. 6 ns pulse width at the third harmonic (355 nm). The incident laser energy was attenuated to a few millijoules per pulse. Time profiles over the wavelength range 300−800 nm were recorded point by point at 10 nm steps using a PC-controlled kinetic absorption spectrometer described earlier.[11] Kinetic traces were recorded in the same fashion at a given wavelength over the relevant time interval.

For determinations of the bimolecular rate constants for oxygen quenching the solutions were saturated in turn with air, argon, and oxygen by bubbling the sample with appropriate gas for several minutes in a cuvette with a Teflon cap equipped with a hypodermic syringe and a small hole to allow egress of gas.

Triplet Extinction Coefficients and Quantum Yields. The relative actinometry method was employed to measure the product $\epsilon_T\Phi_T$ with tetraphenylporphyrin (TPP) as the reference with triplet state quantum efficiency (Φ_T) of 0.82[12] and an extinction coefficient (ϵ_T) at 440 nm of 67 000 M^{-1} cm^{-1}. The sample and reference solutions in toluene were prepared with matched absorptions of ∼0.2 at 355 nm in 10 mm path length cuvettes. The triplet state decay profiles were recorded in air-saturated solutions at 440 nm for TPP and 510 nm for the silicon phthalocyanine compounds. Values of ΔA_{440} and ΔA_{510} were recorded immediate post-pulse (zero time) prior to any decay occurring. The following was employed to calculate $\epsilon_T\Phi_T$ for the unknown (X):

$$\Phi_T^X\epsilon_T^X(510) = \frac{\Delta A_{510}}{\Delta A_{440}}\Phi_T^{REF}\epsilon_T^{REF}(440)$$

The extinction coefficients were determined by the energy transfer method using TPP as the energy transfer donor. A deaerated solution of TPP in toluene with absorbance ∼0.1 at 355 nm bubbled with Ar for several minutes in a cuvette with a Teflon cap equipped with a hypodermic syringe and a small

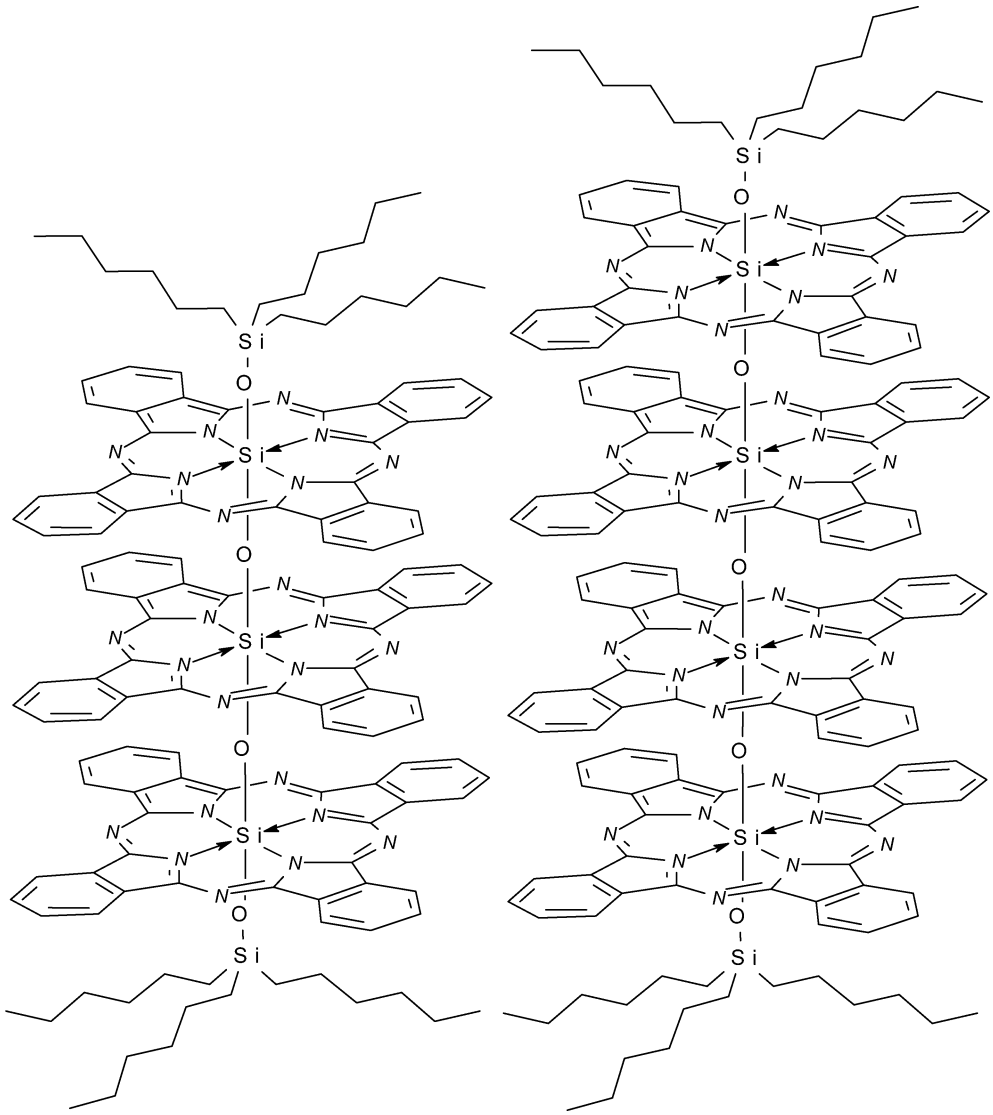

Figure 1. Structures of $(n\text{-}C_6H_{13})_3SiO(SiPcO)_{3and4}Si(n\text{-}C_6H_{13})_3$ (rings rotate freely in solution).

hole to allow egress of gas was employed and the rate constant (k_d) for the decay of TPP triplet in the absence of acceptor was determined. A silicon phthalocyanine (energy acceptor) concentration near 10 μM was used. This proved to be insufficient to capture the whole TPP triplet population and corrections for the unscavenged fractions were necessary. The rate of formation (k_{obs}) of the phthalocyanine triplet was observed at 510 nm, which is an isosbestic point in the TPP transient absorption spectrum. The decay rate of the TPP triplet at 440 nm was recorded, thereby providing the value of ΔA at time zero. The value of ΔA for phthalocyanine triplet at time zero was obtained from fitting of the time profile at 510 nm. To calculate the triplet extinction coefficient, the relationship

$$\epsilon_{510}^{X} = \epsilon_{440}^{TPP}\frac{\Delta A_{510}}{\Delta A_{440}}\cdot\frac{k_d}{k_{obs} - k_d}$$

was employed.[13]

Ultrafast Pump−Probe Measurements. The pump−probe instrument for the ultrafast transient absorption measurements has been described previously.[14] The recent improvements to enhance signal-to-noise characteristics have been communicated elsewhere.[6] In the current experiments excitation was at 620 nm derived from an optical parametric amplifier (Spectra Physics OPA 800).

Results

Ground State Absorption Spectra. The UV−visible absorption spectra of the μ-oxo silicon phthalocyanine trimer and tetramer were measured in toluene solutions at ca. 2 μM concentrations. The normalized spectra are displayed in Figure 2, along with those of $SiPc(OSi(n\text{-}C_6H_{13})_3)_2$ (monomer) and $O(SiPc)_2(OSi(n\text{-}C_6H_{13})_3)_2$ (dimer) for comparison purposes. The trimer and tetramer show significant blue shifts with respect to the dimer and to the monomer in both Q-band and B-band regions. Table 1 summarizes the wavelength maxima for the four species and the spectral shifts (in wavenumbers) with respect to the monomer. It is clear from Figure 2 that the Q-band peaks of the trimer and tetramer are very narrow in the center and have significant unresolved wings on both red and blue sides.

Transient Spectra and Kinetics: Nanosecond and Longer. The transient absorption spectra of the μ-oxo trimer and tetramer (ca. 2 μM) were recorded in degassed solutions (ca. 2 μM) in toluene. The samples were excited using 6 ns laser pulses at 355 nm, and spectra were recorded point by point over the wavelength range 300−800 nm in 10 nm steps. The time dependent transient absorption data for the tetramer are displayed in Figure 3 along with a representative decay profile (Figure 3, inset). Both trimer and tetramer showed similar absorption

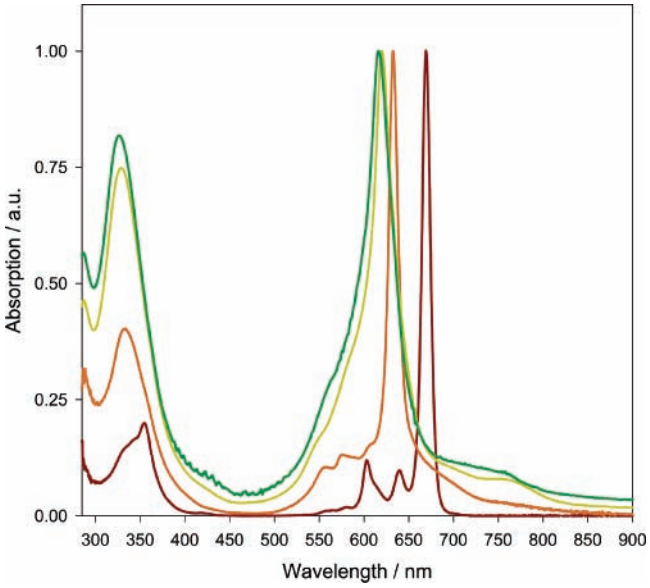

Figure 2. Normalized ground state absorption spectra of the three μ-oxo oligomers and silicon phthalocyanine monomer for comparison: brown, monomer; orange, dimer; light green, trimer; dark green, tetramer.

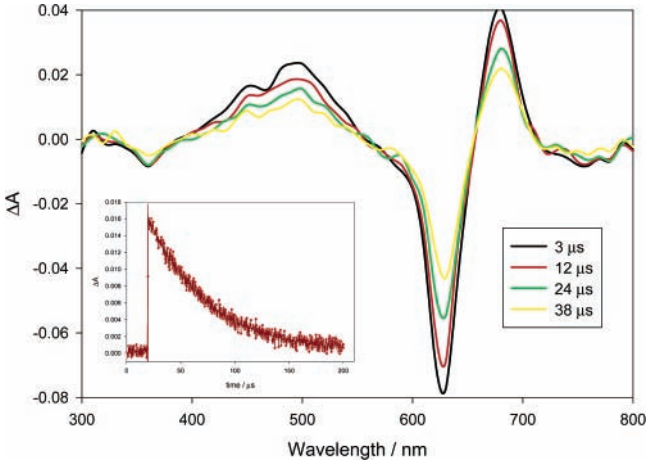

Figure 3. Transient absorption spectra recorded at different times (as shown) after irradiation with a 6 ns pulses at 355 nm of a ca. 2 μm solution of the trimer in toluene. The inset shows the decay profile of the Ar-saturated trimer at 510 nm and the single-exponential fit.

TABLE 1

compound	λ_{max}/ nm	$\Delta\varpi$/ cm^{-1}	ϖ/ cm^{-1}
monomer	668.5		14 958
dimer	632.0	863	15 822
Trimer	620.0	1169	16 129
tetramer	616.0	1273	16 233

features, viz. negative absorption (bleaching) in the Q and Soret band regions, a broad positive absorption feature centered near 500 nm and another positive absorption on the red side of the bleaching band. An isosbestic point was detected between the Q-band bleaching and the positive feature to the red side (near 650 nm). Under the prevailing conditions of argon saturation, the negative and positive absorption features decayed to the prepulse baseline in accord with an exponential rate law. In both compounds the absorption and bleaching kinetics had identical lifetimes and isosbestic points separated the absorption and bleaching features.

The kinetic time profiles changed upon adding oxygen to the solutions. In both compounds addition of O_2 enhanced the

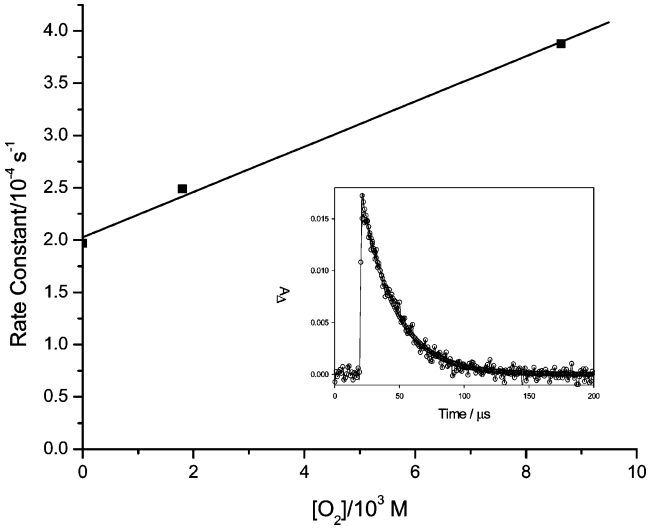

Figure 4. Competition plot of the dependence of the first-order rate constant for quenching of the triplet state of the trimer by oxygen at 20 °C in toluene solution. The bimolecular rate constant is the slope of the plot. Inset: the time profile of the trimer triplet in oxygen-saturated toluene.

TABLE 2

Pc	$\epsilon_{510\ nm}$/ M^{-1} cm^{-1}	τ/ μs	$10^{-6}k_{O_2}$/ M^{-1} s^{-1}	$10^{-9}k_{isc}$/ s^{-1}	Φ_T	E_T/ kcal mol^{-1}
dimer	21 600[a]	116	20	7.8	0.22	19.0
trimer	21 090	51	2.16	26.6	0.114	~17
tetramer	20 500	37	1.51	80	0.094	~17

[a] At 500 nm.

absorption decay and bleaching recovery processes. The bleaching recovery and absorption decay rate constants were first order in oxygen concentration (Figure 4). Bimolecular rate constants for oxygen quenching of the triplet state of trimer and tetramer were found to be 2.16×10^6 and 1.51×10^6 M^{-1} s^{-1}, respectively (Table 2).

Extinction Coefficient and Quantum Yields. To obtain a quantitative picture of the excited state dynamics of the compounds necessitates measuring the extinction coefficients of the triplet−triplet absorption spectra and quantum yields of triplet formation. These experiments were performed by the energy transfer method using H_2TPP as the standard, as described in the Experimental Section. The results obtained are collected in the Table 2 along with the relevant data for the dimer (from ref 6).

Transient Spectra and Kinetics: Subnanosecond. To determine the dynamics of the early events, ultrafast pump−probe absorption experiments were performed. In this experiment, mode locked, amplified Ti:Sapphire laser pulses of ca. 100 fs duration at 620 nm were used to excite solutions of trimer and tetramer in toluene. The transient absorption spectra were monitored using the pump−probe method in which a coherent white light continuum was generated for the probe pulse. The spectra were recorded using a CCD spectrograph, as described in the Experimental Section. Transient absorption spectra at a series of time delays for the trimer are presented in Figure 5 in which a well-defined isosbestic point at 595 nm connects positive and negative absorptions. Similar data for the tetramer are shown in Figure 6. The time profile of the excited state deactivation of the trimer at 525 nm is presented in Figure 7. The decay was exponential with a small nonzero baseline providing a lifetime of 37.6 ± 5 ps. The tetramer showed similar spectra and differed only in lifetime value (12.5 ± 2 ps at 550

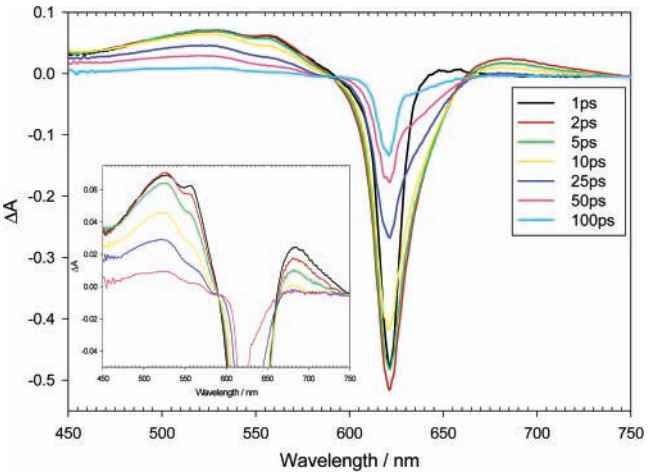

Figure 5. Series of pump−probe transient absorption spectra recorded at different delay times (as shown) after excitation of the trimer solution in toluene with 100 fs pulses at 620 nm. The inset shows the same data with the positive regions enhanced.

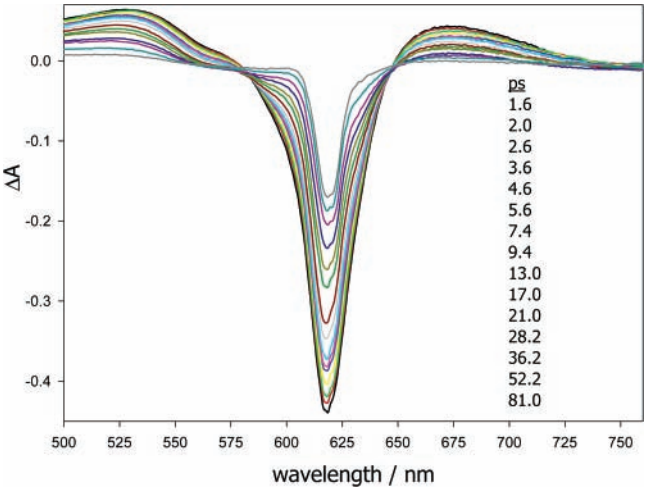

Figure 6. Same experiment as in Figure 5 with the tetramer in place of the trimer.

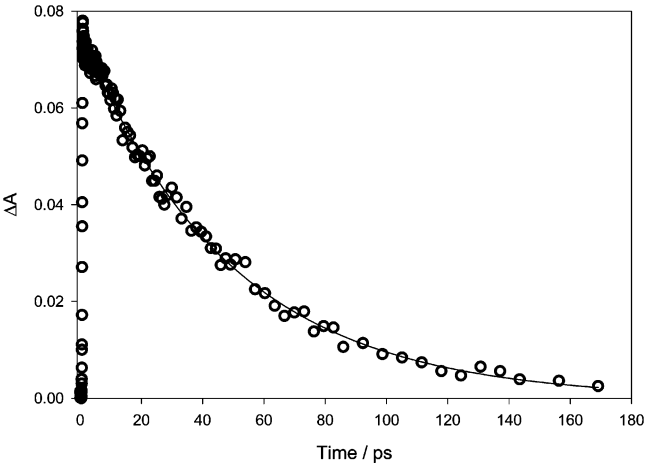

Figure 7. Time profile of the absorption at 525 nm under the same conditions as in Figure 5. The solid curve indicates the monoexponential fit with nonzero baseline.

nm). Figure 5 (inset) shows the existence of twin peaks at the earlier delay times in the 450−600 nm region. Also clearly shown are spectral changes as the delay time increased. The 560 nm peak decayed biexponentially to a nonzero baseline with lifetimes of 5.7 ± 1 and 28.7 ± 3 ps.

SCHEME 1: Synthesis of Oligomers

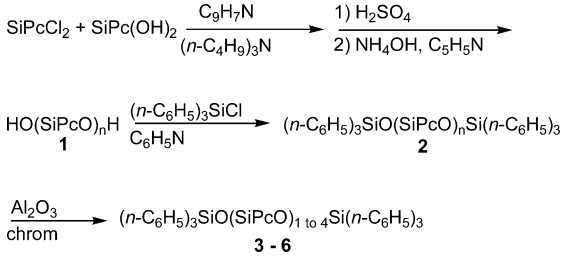

Discussion

Preparative Work. The route used to prepare the oligomers, Scheme 1, utilizes well-established silicon phthalocyanine chemistry.[9,10] Although higher oligomers are undoubtedly produced by this route, they are produced in low yields and evidence for only the pentamer was obtained.

Ground State Spectra. The absorption spectra of the μ-oxo trimer and tetramer (Figure 1) are in good agreement with previously reported data.[10] It is generally agreed that the blue shift of the Q-bands with respect to the monomer is due to an excitonic interaction of the transition dipoles of the coplanar silicon phthalocyanine units having central symmetry along the Si−O−Si axis, with no significant molecular orbital overlap.[15] This excitonic interaction generates a new set of excited states in the dimer, labeled here, $|+\rangle$ and $|-\rangle$. In the dimer the transition from ground state (S_0) to the upper exciton state $|+\rangle$ is allowed and that to the lower exciton state $|-\rangle$ is largely forbidden.[4,16,17]

As Figure 2 shows, the Q-band shift (with respect to the monomer) is greater as the number of phthalocyanine rings is increased. This blue shift is consistent with the molecular exciton model for a linear polymer.[18] This model ignores end effects of monomer units and any interaction between nonneighbor monomer units. It is applicable for dimers and long chain polymers and yields approximations for oligomers (3−10 monomer units).[18]

The other notable characteristics about the oligomer spectra are the blue and red wings at either side of the main Q-band. Such effects have been known for Si−O−Si dimers for a number of years[15,19] and have been attributed to different torsional conformational forms of the dimers. NMR spectra have indicated that the D_{4h} symmetry species is only one of the possible torsional conformations and that, in fact, the macrocycles can rotate freely about the Si−O-M axis.[20] Calculations by Hush and Woolsey[15] lend support to the concept that the dimers can exist in a variety of conformations about the C_4 axis.

Transient Spectra and Kinetics: Nanosecond. Figure 3 shows the transient spectrum changes over the microsecond time scale for the tetramer after excitation with 6 ns pulses at 355 nm. Both trimer and tetramer showed similar spectral features, i.e., negative absorption in the Q and Soret-band regions, a broad positive absorption maximum near 500 nm, and positive absorption on the red side of the ground state bleaching band near 680 nm. The trimer and tetramer transient absorption spectra are comparable with the dimer transient spectra already published.[6] The decay kinetics of the positive bands near 500 and 680 nm were identical for both the trimer ($\tau = 51 \pm 5.5$ μs) and tetramer ($\tau = 37 \pm 4$ μs), indicating that the two bands belong to the same transient species. Further, these two bands are separated from the ground state bleaching band with well-defined isosbestic points, and the bleaching recovery kinetics are identical to the absorption decay kinetics, indicating concomitant behavior, i.e., as the positive absorbing transient

decays, the ground state is repopulated. It is very likely that the transient observable on the nanosecond and longer time scale has a broad continuous absorption between ca. 400 and ca. 700 nm, superimposed upon which is an intense ground state bleaching signal.

As described in Pelliccioli et al.[6] and references therein, the positive absorption near 500 nm can be assigned to the triplet−triplet ($T_1 \rightarrow T_n$) absorption. The appearance of the isosbestic point between positive absorption and ground state bleaching indicated that the species near 500 and 680 nm are responsible for the ground state repopulation without any intermediate entities. Therefore we can conclude that the positive peaks near 500 and 680 nm in both the trimer and tetramer arise from a T_1 to T_n transition. The values of the extinction coefficient and triplet state quantum yields for the three oligomers are collected in Table 2. The extinction coefficients for all three are very close, but the triplet state lifetime and the triplet quantum yield seem to decrease with increasing oligomer length.

Oxygen Quenching of the Triplet State. In the presence of oxygen, the triplet states of the trimer and tetramer decayed exponentially to a zero baseline. The rate constant of the decay was directly proportional to the O_2 concentration, whence the bimolecular rate constant for oxygen quenching could be extracted (Figure 4 and Table 2). It has been demonstrated in several situations[6] that exergonic energy transfer from most triplet states to oxygen occurs with rate constants that are close to 2×10^9 M^{-1} s^{-1}. Rate constant values lower than this are found when the transfer is endoergonic. The values of 2.16×10^6 M^{-1} s^{-1} for trimer and 1.51×10^6 M^{-1} s^{-1} for tetramer found here thus indicate that the energy transfer to $O_2(^1\Delta_g)$ is significantly uphill. Moreover, observations aimed at measuring the 1269 nm luminescence arising from the $O_2(^1\Delta_g)$ to $O_2(\Sigma_g^{3-})$ transition were unsuccessful, indicating that no singlet oxygen was produced during the quenching event. These observations lead to the conclusion that the quenching of the triplet in the presence of O_2 is due to a bimolecular interaction as a result of which the reactants reach the ground state surface directly.

$$^3\mathrm{Pc}^* + \mathrm{O}_2(\Sigma_g^{3-}) \xrightarrow{k_q} \mathrm{Pc} + \mathrm{O}_2(\Sigma_g^{3-})$$

This continues the trend reported for the dimer where the singlet oxygen quantum yield was as low as 0.022, only 10% of the triplet state quantum yield.[6] Knowing that the energy gap for the $O_2(^1\Delta_g) \rightarrow O_2(\Sigma_g^{3-})$ transition is 22.5 kcal mol^{-1} and measuring the equilibrium constant for the reversible energy transfer reaction enabled Pelliccioli et al.[6] to estimate the triplet energy for the dimer at 19.0 kcal mol^{-1}. In the case of the trimer and tetramer, no singlet oxygen formation could be observed, but assuming that the reverse reaction was the same for the dimer and the higher oligomers, and estimating an upper bound for the singlet oxygen formation process allows an approximate value of 17 kcal mol^{-1} to be computed for the triplet energy of the trimer and just slightly lower for that of the tetramer.[21]

The increasing blue shifts with oligomer length in the ground state absorption spectra are consistent with exciton interactions in the cofacial geometry. For triplet states exciton interactions are negligible because transition dipole moments are exceedingly small.[4] However, charge resonance interactions are possible in which the excitation may be regarded as being delocalized over the monomer units in the oligomer.[22] Pelliccioli et al.[6] concluded that such interactions lead to significant energy lowering in the triplet manifold of the PcSi−O−SiPc dimeric entity, causing the energy of the state to be some 2500 cm^{-1} lower than that of singlet oxygen (7870 cm^{-1}). The present work indicates that the trimer and tetramer have triplet energies near to 6000 cm^{-1}, indicating that the charge resonance interactions, like exciton behavior, is enhanced by the longer chains.

Ultrafast Measurements. Figure 5 shows a series of spectra obtained after 620 nm excitation of a solution of the trimer (∼10 μM) in toluene in the pump−probe spectrometer. Figure 6 shows the result of an identical experiment for a similar solution of the tetramer. The two compounds show similar behavior and the data for the trimer will be discussed in detail, keeping in mind that the tetramer follows similar patterns, except where indicated. In Figure 5, at 2 ps postexcitation a broad positive absorption is seen to extend throughout the visible spectral region. This is interrupted with a negative absorption (bleaching) signal having an extremum at 620 nm, the peak wavelength of the ground state absorption band (Figure 2). This bleaching is identified as being the result of depopulation of the ground state by the excitation pulse. Moreover, as the time delay between pump and probe pulses increased beyond 2 ps, isosbestic points were observed at 590 and 660 nm, between the positive and the negative absorption regions. This behavior indicates that the entity responsible for the positive absorption bands is converting into the ground state as it decays. Close inspection of Figure 5 (inset) reveals that the absorption on the blue side of the 590 nm isosbestic point is composed of a pair of weakly resolved peaks at 520 and 560 nm, respectively. As the delay time increases, it can be seen that the 560 nm feature decays more rapidly than the 520 nm feature. The absorption band around 520 nm decays exponentially to a nonzero baseline with lifetime of 37.6 ps. This is identified as the rate of intersystem crossing from the lowest exciton state into the triplet manifold. The 560 nm feature decays biexponentially to a nonzero baseline and has lifetimes of 5.8 and 28.7 ps. It is very likely that the 37.6 ps lifetime at 520 nm and the 28.7 ps component at 560 nm represent the decay lifetime of the same species within the uncertainty of the measurements. In the case of the SiPc μ-oxo dimer, Pelliccioli et al.[6] reported spectral features in the 500−600 nm region similar to those seen here (Figure 5). In that work these features developed fully over several tens of picoseconds, whereas here they were developed during the instrument rise time (ca 300 fs). Pelliccioli et al. attributed this spectrum to the lower exciton state of the dimer, which transformed via an intersystem crossing process into the triplet manifold with a lifetime of 128 ps. By analogy, it is concluded that a similar situation exists in the trimer (and tetramer) entity, with the difference that here at least some of the processes (vide infra) leading to the development of the lowest exciton state are completed within the instrument rise time and the intersystem crossing process is significantly more rapid for the trimer. These rate enhancements from dimer to trimer are not unexpected given that the lowest band of exciton states in the trimer will be lower in energy than the lower one of the two-dimer state; thus the energy gap to the triplet is presumably less. Also, the fact that there are more states in the trimer exciton band means that the state to state gaps will be smaller and the relaxation from the state populated by photon absorption will become more facile. However (Table 2), it is seen that these enhanced decay constants are paralleled by decreases in the yield of the T_1 state as the oligomer length increases. This, together with the small yield values, implies that nonradiative and non-ISC processes are also becoming of increasing importance to the deactivation events as the oligo length increases. Figure 8 shows the early time profiles of the absorption signals at three wavelengths, two to the blue side and one to the red side of the ground state bleach. The superimposition of these (with normalization) clearly

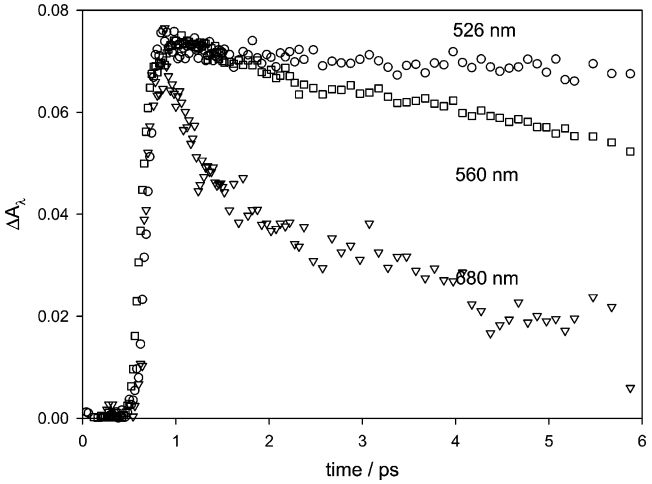

Figure 8. First few picoseconds of the time profiles recorded at the indicated wavelengths under the conditions of Figure 5 (see text).

demonstrates the temporal differences in these spectral ranges. At 526 nm the data shown are the early phase of the ISC process from the lowest exciton state, referred to above. The 560 nm data are part of the early component at that wavelength having a lifetime of 5.76 ps (vide supra). The figure shows clearly that the decay at 680 nm is not a single component; a two exponential fit shows lifetimes of 490 fs and 9.0 ps. At the same time it is important to note that at no wavelength was it possible to discern any growth process slower than the instrument response. In the Pelliccioli et al. paper the early (ca 10 ps) processes were attributed to torsional/vibrational relaxation in the exciton band.

In the μ-oxo oligomers, a single covalent Si−O−Si linkage connects the adjacent π-planes. Torsional motions about these bonds generate an ensemble of conformations in which the D_{4h} symmetry is broken. This symmetry breaking is responsible for the significant extinction in the red and blue wings of the 0,0 transition (Figure 2). Thus excitation of the dimers and higher members within the intense 0,0 band leads to population of the highest-lying exciton state, $|+\rangle$, largely but not exclusively in D_{4h} symmetry. This will be followed very rapidly by nonradiative crossing to an upper torsional/vibrational state of one of the lower-lying exciton states, which loses excess energy with a 10 ps relaxation time to generate the thermally equilibrated $|-\rangle$ state, the immediate precursor of the triplet state. The processes showing 5.76 and 9.0 ps lifetimes are very likely to be the temporal signatures of such torsional/vibrational events. It is also possible that the 490 fs decay at 688 nm is another, although it cannot be completely ruled out that this is due to electric dipole transitions between the exciton states. Such transitions are thought to occur on such time scales as demonstrated in ultrafast absorption experiments, which have revealed that interexciton state relaxation occurs in a few tens of femtoseconds in allophycocyanine trimers[23] and within 500 fs in porphyrin arrays[24] where the exciton splitting is near 3000 cm^{-1}.

The only major difference shown by the tetrameric species was that the process assigned to intersystem crossing occurred with a lifetime of 12.5 ps.

Acknowledgment. This work has been supported in part by funding from the National Institutes of Health grants CA 46281, 48735, and 91027. T.S. is grateful to the McMaster Foundation (BGSU) for a research assistantship.

References and Notes

(1) Ferencz, A.; Neher, D.; Schultz, M.; Wegner, G.; Viaene, L.; Schryver, F. C. D. *Chem. Phys. Lett.* **1995**, *245*, 23.

(2) Leznoff, C. C., Lever, A. B. P., Eds. *Phthalocyanines: Properties and Applications*; VCH Publishers: New York, 1996; Vols. I−IV

(3) Manas, E.; Spano, F. C.; Chen, L. X., *J. Chem. Phys*. **1997**, *107*, 707.

(4) Kasha, M. *Radiat. Res*. **1963**, *20*, 55.

(5) Oddos-Marcel, L.; Madeore, F.; Bock, A.; Neher, D.; Ferencz, A.; Rengel, H.; Wegner, G.; Kryschi, C.; Trommsdorff, H. P. *J. Phys. Chem*. **1996**, *100*, 11850.

(6) Pelliccioli, A. P.; Henbest, K.; Kwag, G.; Carvagno, T. R.; Kenney, M. E.; Rodgers, M. A. J. *J. Phys. Chem. A* **2001**, *105*, 1757.

(7) Ern, J.; Bock, A.; Oddos-Marcel, L.; Rengel, H.; Wegner, G.; Trommsdorff, H. P.; Kryschi, C. *J. Phys. Chem. A* **1999**, *103*, 2446.

(8) (a) Soncin, M.; Busetti, A.; Fusi, F.; Jori, G.; Rodgers, M. A. J. *Photochem. Photobiol*. **1999,** *69*, 708. (b) Busetti, A.; Soncin, M.; Reddi, E.; Rodgers, M. A. J.; Kenney, M. E.; Jori, G.. *J. Photochem Photobiol, B: Biol*. **1999**, *53*, 103.

(9) Wheeler, B. L.; Nagasubramanian, G.; Bard, A. J.; Schechtman, L. A.; Dininny, D. R.; Kenney, M. E. *J. Am. Chem. Soc.* **1984**, *106*, 7404−7410.

(10) DeWulf, D. W.; Leland, J. K.; Wheeler, B. L.; Bard, A. J.; Batzel, D. A.; Dininny, D. R.; Kenney, M. E. *Inorg. Chem.* **1987**, *26*, 266−270.

(11) Rihter, B. D.; Kenney, M. E.; Ford, W. E.; Rodgers, M. A. J. *J. Am. Chem. Soc*. **1990**, *112*, 8064.

(12) Venedictov, V. A.; Krasnovsky, A. A. *Zh. Prokl. Spektrosk*. **1982**, *36*, 152.

(13) Carmichael, I.; Hug, G. L. *J. Phys. Chem. Ref. Data* **1986**, *15*, 1.

(14) Nikolaitchik, A. V.; Korth, O.; Rodgers, M. A. J. *J. Phys. Chem. A* **1999**, *103*, 7587.

(15) Hush, N. S.; Woolsey, I. S. *Mol. Phys*. **1970**, *21*, 465.

(16) Kasha, M.; Rawls, H. R.; El-Bayoumi, A. *Pure Appl. Chem*. **1965**, *11*, 371.

(17) A referee points out that vibronic transitions from the lowest exciton level have nonvanishing oscillator strength and that the lack of significant fluorescence from that level must be the result of rapid nonradiative deactivation.

(18) McRae, E. G.; Kasha, M. *Phys. Process Rad. Biol*. **1963**, 23−42.

(19) Kane, A. R.; Sullivan, J. F.; Kenny, D. H.; Kenney, M. E. *Inorg. Chem*. **1970**, *9*, 1445.

(20) Esposito, J. N.; Lloyd, J. F.; Kenney, M. E. *Inorg. Chem*. **1966**, *5*, 1979.

(21) A referee correctly points out that it is extremely unlikely that the two excited states (^{3}Pc* and $O_2(^1\Delta_g)$) are in fact in thermodynamic equilibrium under the experimental conditions. Were this so it would have been manifest as a biexponential decay of the ^{3}Pc* absorption, as found for the μ-oxo dimers by Pelliccioli et al.[6] Here we have made an (incorrect) assumption of equilibrium to obtain *approximate* values of the triplet energies of the trimer and tetramer. The O_2-quenching rate constants themselves, being an order of magnitude lower than that for the dimer (Table 2) already indicate that the triplet energies of the trimer and dimer triplet states are significantly lower than that of the μ-oxo dimer.

(22) Ishii, K.; Yamauchi, S.; Ohba, Y.; Iwaizumi, M.; Uchiyama, I.; Hirota, N.; Maruyama, K.; Osuka, A. *J. Phys. Chem*. **1994**, *98*, 9431.

(23) Edington, M. D.; Riter, R. E.; Beck, W. F. *J. Phys. Chem*. **1996**, *100*, 14206.

(24) Cho, H. S.; Song, N. W.; Kim, Y. H.; Jeoung, S. C.; Hahn, S.; Kim D.; Kim, S. K.; Yoshida, N.; Osuka, A. *J. Phys Chem. A* **2000**, *104*, 3287.